Micro-CT in Osteoporosis Research

7

Szandra Körmendi, Bálint Vecsei, Kaan Orhan, and Csaba Dobó-Nagy

Abbreviations

BALP	Bone-specific alkaline phosphatase
BMC	Bone mineral content
BMD	Bone mineral density
BRONJ	Bisphosphonate-related osteonecrosis of the jaw
BS/BV	Bone surface/bone volume ratio
BV	Bone volume
BV/TV	Percentage of bone volume
Ca.Dm	Canal diameter
Ca.Sp	Canal separation
Ca.V	Canal volume
Ca.V/TV	Canal porosity
CKD	Chronic kidney disease
Conn.D	Connectivity density
Cr. BMD	Cortical bone mineral density
CS	Canal surface
Ct.Po	Cortical porosity
Ct.Th	Cortical thickness
CTX	C-terminal telopeptide fragment of type I collagen
DA	Degree of anisotropy
DEXA, DXA	Dual energy X-ray absorptiometry
DPD	Deoxypyridinoline
FEA	Finite element analysis
L1–L4	Lumbal 1–4 vertebra
Lc.N/TV	Lacunar density
Lc.V/TV	Lacunar porosity
NTX	Type I collagen cross-linked N-telopeptide
OC	Osteocalcin
OPG	Osteoprotegerin
OVX	Ovariectomized
PINP	Procollagen type 1 amino-terminal propeptide
PTH	Parathyroid hormone
ROI	Region of interest
SAMP6	Senescence-accelerated mouse P6
SHAM	Sham-operated
SMI	Structural model index
Tb.N	Trabecular number
Tb.Pf	Trabecular pattern factor

S. Körmendi (✉) · B. Vecsei
Faculty of Dentistry, Department of Prosthodontics, Semmelweis University, Budapest, Hungary
e-mail: kormendi.szandra@dent.semmelweis-univ.hu; vecsei.balint@dent.semmelweis-univ.hu

K. Orhan
Faculty of Dentistry, Department of Dentomaxillofacial Radiology, Ankara University, Ankara, Turkey

Faculty of Medicine, OMFS IMPATH Research Group, Department of Imaging and Pathology, University of Leuven, Leuven, Belgium

Oral and Maxillofacial Surgery, University Hospitals Leuven, University of Leuven, Leuven, Belgium
e-mail: knorhan@dentistry.ankara.edu.tr; kaan.orhan@uzleuven.be

C. Dobó-Nagy
Faculty of Dentistry, Department of Oral Diagnostics, Semmelweis University, Budapest, Hungary
e-mail: dobo-nagy.csaba@dent.semmelweis-univ.hu

K. Orhan (ed.), *Micro-computed Tomography (micro-CT) in Medicine and Engineering*,
https://doi.org/10.1007/978-3-030-16641-0_7

Tb.Sp	Trabecular separation
Tb.Th	Trabecular thickness
TMD	Tissue mineral density
TRACP-5b	Tartrate-resistant acid phosphatase 5b
TV	Tissue volume
VOI	Volume of interest

7.1 Introduction: Osteoporosis

Osteoporosis is a systemic bone disease that occurs along with low bone density, loss of bone and the lesion of the microarchitecture of bone tissue, resulting in an increase in bone fragility.

Around 200 million people are affected in civilized societies worldwide, and a significant surge in this number can be expected in the future. An even more alarming data is that only a low percentage of patients will be getting treated. This number is around 10%, although we know that the average lifespan of a woman with osteoporosis is 4 years less than of someone not having this disease. Two thirds, according to some other data three quarters of all patients are women which can derive from various presumed reasons. Firstly, the initially thinner and lower-weight bone structure [1] can be mentioned; secondly, women due to postmenopausal oestrogen deficiency are more prone to bone loss; and thirdly, in almost all populations, women live longer than men so their proportion with the progression of age grows at the expense of men [2]. All these data along with the fact that following cardiovascular diseases, musculoskeletal disorders impose the greatest burden on the economy and on the society contributed to the fact that the World Health Organization initiated by Swedish orthopaedists announced the Bone and Joint Decade first between 2000 and 2010 and then the second time between 2011 and 2020. The initiative joins together 65 countries, and it is supported by 750 associations. Its aim is to reduce the economic and social burden caused by musculoskeletal diseases by improving prevention, diagnosis and treatment of these diseases.

Types of osteoporosis can be classified in different ways: based on the dynamics of bone building and bone degeneration, we differentiate low, normal and high turnover osteoporosis; secondary and primary types can also be differentiated depending on the fact if the osteoporosis is a result of another primary disease or it is a separate clinical picture; also there is Type I (postmenopausal) and Type II (senile) classifications.

7.2 Role of Micro-CT in Osteoporosis Research

Micro-CT is a widespread tool used for observing the changes in the microarchitecture of the bone tissue; thus the pathology of osteoporosis and the effects of treatments can be well examined by it. It is primarily used in in vitro examinations, but there is opportunity for in vivo experiments too. The sample used for the examination can be of human as well as of animal origin (Fig. 7.1).

7.2.1 Human Researches

In micro-CT studies, due to the size of the sample, mainly in the case of in vivo studies, they are mostly animal-derived, but we can also find many human studies. The importance of selecting the location of sampling is shown by the research of Eckstein and his colleagues. One hundred sixty-five samples taken from human cadavers were processed using micro-CT. The locations of the sampling were the distal radius, the femoral neck and trochanter, iliac crest, calcaneus and second vertebral body, where in each case the volume of interest (VOI) was a 6-mm-diameter and 6-mm-long cylinder examined with a 26 μm voxel. At the distal radius and at the femoral neck, the trabecular bone had a more plate-like structure, thicker trabeculae, higher trabecular number (Tb.N), smaller trabecular separation (Tb.Sp), higher connectivity and higher degree of anisotropy (DA) by men than by women. The trochanter shows more plate-like and thicker trabeculae by men. The calcaneus, the iliac crest and the lumbal 2 (L2) vertebra show no difference between the two genders [3].

In 2003, Dufresne et al. examined the effect of risedronate in placebo-controlled test on the

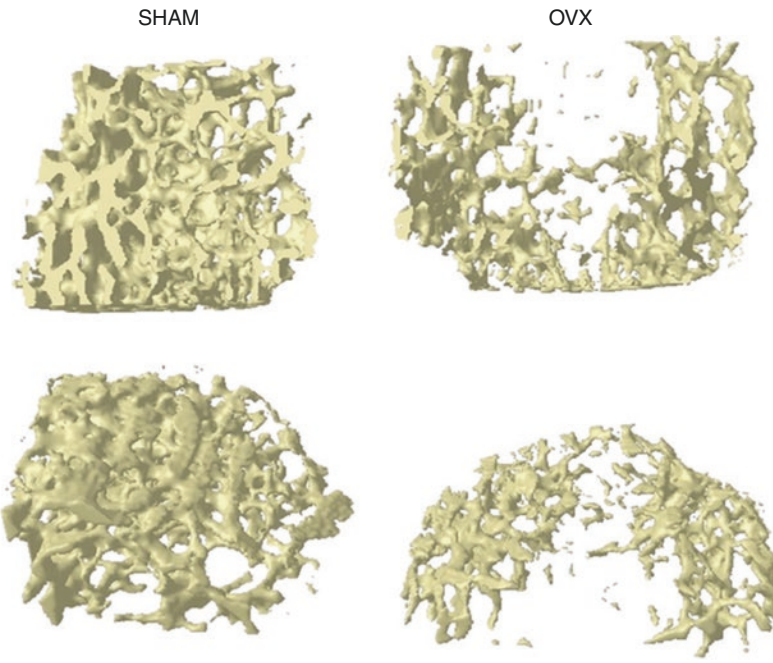

Fig. 7.1 Representative samples from mice femur in the case of ovariectomy or sham operation

samples taken from the hip bone. After 1 year of treatment, it was found that the percentage of bone volume (BV/TV) decreased by 20%, the Tb.N decreased by 14% and Tb.Sp increased by 13% compared to the baseline in the group taking placebo, while by the ones taking risedronate, it did not appear to have significant differences compared to baseline values. However, during this time, the bone mineral density (BMD) measured with dual energy X-ray absorptiometry (DEXA) in the lumbar spine section decreased only by 3.3% among placebo users [4].

Arlot et al. treated postmenopausal patients with strontium ranelate or with placebo in a 3-year follow-up study. With the help of micro-CT, they analysed transiliac bone biopsy at the end of the research, and it was found that compared to the placebo group by the strontium ranelate consumers, structural model index (SMI) significantly improved and Tb.Sp significantly decreased, while cortical thickness (Ct.Th) and Tb.N increased [5].

The effectiveness of treatment with human parathyroid hormone (PTH) was also tested in placebo-controlled research; in a micro-CT analysis of the sample obtained with hip biopsy, there it was found that BV/TV was 44%, Tb.N 12%, and trabecular thickness (Tb.Th) 16% higher compared to the values of the placebo group at the end of the 18-month-long treatment [6].

Yamashita-Mikami et al. examined the bone structure of the alveolar spongiosa taken from the site of implants to be implanted in place of the molars or premolars of the lower jaw among pre-, post- and late postmenopausal women with micro-CT. Besides that, they also examined bone turnover markers (type I collagen cross-linked N-telopeptide (NTX), bone-specific alkaline phosphatase (BALP), osteocalcin (OC), deoxypyridinoline (DPD)). The BV/TV was significantly smaller, the trabeculae were more separated and more rod-like at the postmenopausal group than in the premenopausal and all bone parameters showed correlation with at least one bone turnover marker [7].

7.2.2 Rat Studies

Because none of the animal models are fully suitable for modelling osteoporosis, since 1994 FDA requires any potential new therapy to be verified

in experiments conducted on at least two different animal species before proceeding further [8]. Osteoporosis models can be created medically (e.g. dosage of oestrogen receptor antagonist [9], gonadotropin release hormone agonist [10]) or surgically. However, besides these, an immobilization model (created surgically, e.g. with neurectomy [11] or with tenotomy [12], or in a conservative way, e.g. with hindlimb [13]), or a model created by interfering in their nutrition (e.g. a low-calcium diet [14]), can also be found in the literature [15]. The ovariectomized rat model was used even before 1973, and then in 1992 it was confirmed that it might be useful in modelling postmenopausal osteoporosis [16]. This model, along with its known errors, represents the gold standard even today. Surgical techniques can also be of several types: both ventral or dorsal approaches are possible [17] (Fig. 7.2). Techniques can also be combined (e.g. simultaneous application of ovariectomy and low doses of calcium intake [18]).

Caution should be taken however when choosing the age of the animals, since with age the modelling changes into the remodelling in cases of both spongiosa and cortical in the rats' skeletal system [19]. Studies show that the examination of remodelling is possible in rats after 12 months of age in cases of the lumbar vertebrae and the tibia proximal metaphysis, because by this time this is the dominant activity in the case of the spongiosa and the cortical [20]. As long as modelling dominates, areas adjacent to proximal tibia epiphysis nearby the growth plate cannot be used for densitometry, tomography or histomorphometry, since length growth can still be experienced in the bones. In female rats this process ends in the case of tibia by the age of 15 months and in the case of lumbar vertebrae by the age of 21 months [20]. Bone loss does not develop at the same pace at different test locations in the spongiosa: 14 days after ovariectomy by the tibia proximal metaphysis; 30 days after by the femoral neck; and 60 days after by the body of lumbar vertebrae, a significant change can be seen. On the contrary after the ovariectomy, the thickness of the cortical bone decreases significantly, in 180 days in the case of the tibia and 90 days in the case of the femur [20]. The rate of bone loss in respect of the whole organism is also of altering dynamics: rapid bone loss is experienced in the first 100 days. This is followed by an intermediate period where, at an osteopenia level, a relative stabilization occurs in the spongiosa and then after 270 days a slower bone loss is experienced [21]. When analysing the cortical bone, the fact that for a long time Havers remodelling could not be demonstrated in rodents posed a problem. It can be experienced that the cortical increases from the periosteum's side and gets thinner from the endosteum side [22]. Further studies have confirmed that Havers system can be found also in the rats' cortical: they are large, highly interconnected and irregular in the endosteal region, while the canals in the periosteal region are straight and small [23].

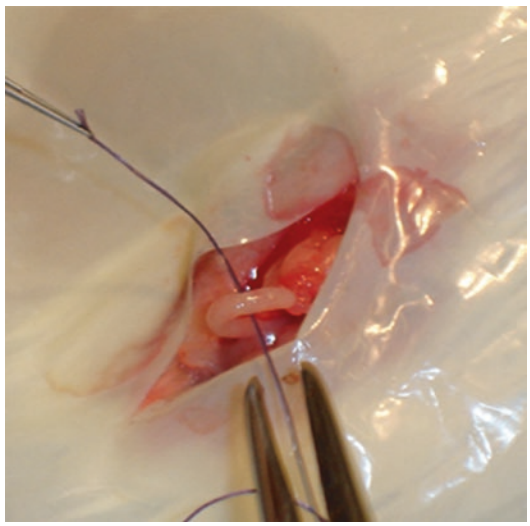

Fig. 7.2 The dorsal ovariectomy technique

Micro-CT is suitable for both in vivo and in vitro examinations in the case of animals this size, as well as several types of sampling places can be used: may this be in the area of the tibia, femur, vertebrae, and mandible.

It was an in vivo examination of Brouwers et al., when they were examining the parathyroid hormone (PTH) treatment's effects in an ovariectomized (OVX) rat model. Immediately after the surgery and then on the 8th, 10th, 12th and 14th week, micro-CT examinations were conducted

under general anaesthetic, in order to cross-reference the proximal tibia meta- and its epiphysis's microstructure. At both areas the growth of the Tb.Th was found as an effect of the therapy. Tb.N grew only in the epiphysis during the time of the longitudinal examination. It was found, therefore, that the two areas react differently to the therapy and firstly bone is to be formed where due to the increased force it is most necessary and only after that at all other surfaces. During the PTH treatment, the cortical bone mass was continuously increasing [24], in accordance with other studies [25].

Dai et al. studied the changes of the alveolar bone in the area of the maxilla in the ovariectomized rat model in vitro. Twelve weeks after the ovariectomy and the sham-surgery (SHAM), the animals were examined, and their maxilla was removed; in order to examine the alveolar bone between the roots of the upper first molar by using micro-CT, a histological examination was also performed. Compared to the BMD, BV/TV and Tb.Th values of the sham-operated group, significantly smaller values were measured at the ovariectomized group. Based on their results, it can be concluded that changes created during ovariectomy can be observed in the maxilla spongiosa the same way like in other bones [26].

Ovariectomized rat models are not only used in micromorphological investigations, but most of the time, biomarkers are also examined along with the aforementioned. This is how it happened in Yoon et al.'s in vitro research, where OC and BALP levels were examined in the serum, which are the sensitive indicators of bone formation, and C-telopeptide of type I collagen (CTX), which is the marker molecule of bone degradation. They found that in the OVX group compared to the SHAM group, a 75.4% higher level of osteocalcin and a 72.5% higher level of CTX level were detected. The increased values of resorption markers indicate the activation of bone resorption in postmenopause, which can be explained by oestrogen deficiency. Bone formation increases due to the elevated number of bone building, starting in the bone lacuna. The osteoporotic bone develops because the balance among these processes shifts. As a result of all these changes, an osteoporotic bone was found, in this case, while the L4 vertebra was examined and mechanical testing was done. In the case of the spongiosa, there was a significant difference between the groups in respect of the Tb.Th, BV/TV and the Tb.Sp, as well as in the case of the cortical bone mineral density (Cr.BMD) [27].

Besides studying the spongiosa, examining the cortical bone keeps gaining greater and greater importance. By using the ovariectomized rat model, Sharma et al. have also studied the spongiosa and the cortical bone structures on the tibia proximal meta- and epiphysis. In line with most of studies, they found that the BV/TV, Tb.Th and Tb.N significantly decreased in the OVX group in respect of the spongiosa, while Tb.Sp and SMI significantly increase. In respect of the cortical, they found that vascular canal porosity (Ca.V/TV) and canal diameter (Ca.Dm) in both the anterior and the posterior region increase in the OVX group, which may contribute to the increased fragility of the osteoporotic bones. In contrast, lacunar porosity (Lc.V/TV) and lacunar density (Lc.N/TV) did not show significant differences between the groups [28].

Bone lesions developed due to oestrogen deficiency were studied in rats' mandible by Ames et al. They found that in the OVX group in the alveolar bone, the variability of the value of tissue mineral density (TMD) is greater than in the control region, which was designated to represent the bone part of the mandible, which is not an alveolar bone, and neither the internal nor the external borders. Oestrogen deficiency increases the level of bone remodelling, and consequently, the variability of TMD also increases. The variability in the alveolar bone increased even more compared to this, presumably due to the chewing, what makes bone remodelling here quite active anyway [29].

The cortical of the mandible in the ovariectomized rats was found significantly thinner by Yang and his colleagues compared to the sham-operated animals. However, 12 months were required for this change [30].

Mavropoulos et al. compared the microarchitecture and bone mineral density (BMD) of the mandible and the proximal tibia. The rats were

ovariectomized or sham-operated and were pair-fed isocaloric diets containing either 15% or 2.5% casein. The animals were given 100 IU/kg body weight vitamin D in peanut oil every day. Seventeen weeks after the surgery, blood was sampled to determine the IGF 1 and OC levels, and they were exterminated. They worked with a 16 μm voxel size in the case of both bones. The mandible VOI was drawn between the roots of the molars and the root of the incisor. The following differences were found: in the members of the SHAM group by a low protein intake, the mandible BV/TV decreased with 17.3%, and the tibia BV/TV decreased with 84.6%. By normal protein intake in the OVX group, the decrease of the mandible BV/TV was 4.9%, as opposed to the 82% decrease of the tibia ($p < 0.001$). A possible explanation of the deviation may be that the mandible's alveolar bone structure is stimulated the continuous chewing, with this protecting the microstructure of this area [31].

Kozai et al. were investigating the impact of the glucocorticoids on the bone structure on the mandible and femur. BMD values were measured by pQCT in both bones. They were also analysing the structure of the spongiosa (voxel size 32 μm) from the first molar root through 100 slices by micro-CT. They found a strong correlation between the mandibular and femoral cortical bone mineral content (BMC): steroid treatment significantly reduces the value of the BMC and the thickness of the cortical in the mandible and the diaphysis of the femur. At the same time, in the trabecular structure of the mandible, no significant changes were observed. The microstructure of the femur was not investigated [32].

Blazsek et al. created an interesting rat model where implants were placed in tail vertebra and treated with aminobisphosphonate. They published a surprising result that the rat tail vertebra was poor in the bone marrow parenchyma but rich in bone forming and resorbing cells. This means that rat tail vertebra is an ideal microenvironment in preclinical investigation where drug affecting bone metabolism can be examined without drug interactions with bone marrow cells just like in the mandible [33].

In light of the above-mentioned researches, it can be seen that within even a single bone, the change of the bone structure can be differing, in osteoporosis models created in different ways.

7.2.3 Mice Studies

Among all animal models, the mouse model is the second most common in osteoporosis research. But while in most rat studies, we meet examinations of the micromorphological changes caused by ovariectomy and consequential oestrogen deficiency, genetically modified mice experimental researches are carried out more frequently among mice. Experiments are usually done on young, 8-week-old mice. Mice do not develop menopause, but as they grow older, they eventually become acyclic. Due to their extremely diverse genetic properties by each mice species, slightly different bone physiological characteristics can be seen.

The bone structure of mice responds similarly to ovariectomy as rats: for example, the stock loss of spongiosa in the proximal metaphysis of tibia is 50% in 5 weeks at Swiss-Webster mice [34]. C57BL/6J is another commonly used mice type. The increase of the femur ends in the 6th–7th month. However, the increase of the intramedullary and the deceleration of bone building are already common at 12-week-old mice (corresponding 40 human years), and these processes result in thinner cortex [35]. Glatt et al. also call attention to the fact that in this tribe the BV/TV value reaches its maximum in the metaphysis of bones when the animals are in 6–8 weeks of age. From that point there is a slow but continuous decrease during their aging even without any bone metabolism influencing factors [36]. However, the cortical bone mass of BALB/c mice does not start to decrease until they reach the age of 20 months [37]. Senescence-accelerated mouse P6 (SAMP6) is used for the modelling of senile osteoporosis. This is the species that attracts attention because microscopic changes in the trabecular bone structure of vertebrae can be observed earlier than in the spongiosa of tibia and femur, but the bone changes of the cortical are

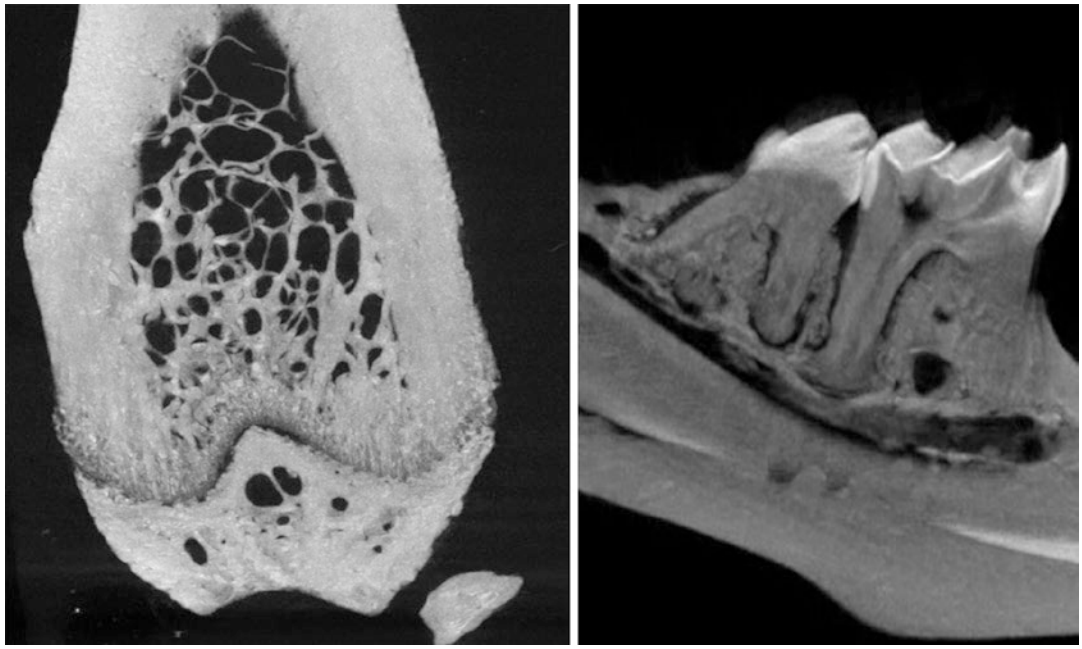

Fig. 7.3 Several types of sampling place (e.g. mouse femur and mandible)

not significant compared to SAMR1 mice of the same age [38].

The femur [39], tibia [38], lumbar vertebra [40] and less often the mandible [41] are the most commonly investigated areas in the case of spongiosa in mice as well (Fig. 7.3).

Sheng et al. examined the effect of zoledronate on osteoprotegerin-deficient mice. Mice received zoledronate or the medium for 4 weeks. BALP and tartrate-resistant acid phosphatase 5b (TRACP-5b) levels were determined from serum with ELISA, and after that the animals were exterminated and the mandible and tibia were removed. Values of BALP and TRACP-5b of KO mice were significantly higher than the ones of the wild type or ones that had received zoledronate. As an effect of zoledronate treatment, high values of BALP and TRACP-5b decreased among KO mice. Both bones were examined using 7-μm-wide voxel size. VOI expanded from the mesial edge of first molar until the distal edge of third molar during the examination of mandible spongiosa, except the teeth and the cortical. A 1.5-mm- X 1.5-mm-wide area was marked out between the lower and the upper barrier on the buccal side of the mandible body during the examination of the cortical. In the case of the KO mice in the mandible, the BV/TV by 31%, Tb.Th by 60%, connectivity density (Conn.D) by 66% and Tb.N by 21% became lower, while the bone surface/bone volume ratio (BS/BV) by 61%, Tb.Sp by 37% and SMI by 114% became higher than in the wild type. In the case of the tibia in KO mice, BV/TV by 93%, Conn.D by 87% and Tb.N by 88% became lower, while SMI became higher by 82% than in wild type. Porosity grew dramatically in the mandible cortical region of KO mice. Lower involvement of the mandible spongiosa in the alveolar area was seen compared to long bones [42].

Six weeks after the ovariectomy and sham surgery of C57BL/6 mice, a 0.8-mm-diameter-wide cortical bone defect was created into the middle diaphysis of the right femur of those mice that were not exterminated. Its changes then were examined in vivo on the 0, 3, 7, 10, 14 and 21 days after the surgery. When these animals were exterminated as well, procollagen type 1 amino-terminal propeptide (PINP) and CTX with

ELISA were determined, and several expressions of more genes were also investigated (i.e. type I collagen, OC). In vivo micro-CT analysis gave the result that bone volume fraction was significantly lower in the defect and intramedullary areas in the OVX group between day 10 and 20. It seems that intramembranous ossification was damaged in the osteoporosis caused by the OVX [43].

7.2.4 Other Animal Models in Osteoporosis Research

Most commonly used postmenopausal animal models were elaborated on rodents which usually means the ovariectomization of the animals. However, these models are often criticized in respect of what kind of significant differences there are between rodents' and humans' bone metabolisms. Critics firstly emphasize the fact that rodents don't have menopause, so it is artificially created for the experiment, and they also differ in their remodelling. That is why, less often though, there are a few researches done on other mammals too. The execution of these is more complicated, and their process time is longer than by rodent models.

Not surprisingly, primates are very similar to humans in respect of hormonal and bone structural changes. These animal species have similar menstruation cycles to humans, and they can reach menopause, only at a much later age [44]. The ovariectomized or sham-operated cynomolgus apes were selected as subjects of the experiment by Binte Anwar et al. Seventy-six weeks after the surgeries, the mandibles and L2–L4 vertebrae were scanned, and the microarchitecture of the area between the second molar and of vertebrae was compared. SMI growth was found in the alveolar bone of the OVX group, and an increasing number of pores were found towards the top of alveolus. A positive correlation between the damage in the structure of the alveolar bone and the microarchitectural condition of the vertebrae was also detected, which observation is of great significance from a parodontological aspect [45].

Effects of drugs used in osteoporosis are being tested on ovariectomized models of cynomolgus apes, for example, the romosozumab by Ominsky et al. [46]. The developed OVX model was applied on rhesus apes [47] and on baboons [48], especially for the micro-CT investigation of lumbar and thoracalis vertebrae's micromorphology. During the test done on baboons, tight correlation was observed between the histological and micromorphological changes of vertebra T12; however, histology was determined as a more sensitive process than micro-CT, at least when the number of cases is low [48]. It must be taken into account that these models require animals aged 8–22 years, and the duration of experiments is 12–24 months.

Minipigs have been used for a long time in various ways in the research of osteoporosis [49] or bisphosphonate-related osteonecrosis of the jaw (BRONJ) [50] research. The advantage of the pig model is they have a well-developed Havers canal system and their oestrous cycle duration is approx. 20 days, but a disadvantage is the relatively low amount of data available of the ovariectomized model [44]. Attention is being drawn in the case of model OVX that while with cynomolgus apes the animals should be older than 9 years, when the operation takes place, minipigs can be operated when they are only 10–18 months old. When testing different medicines, it should be taken into account that a 16 months' dosage at minipigs and cynomolgus apes equals 4 years in the case of human testing [51].

Bone resorption and formation markers raise significantly in 3–4 months at sheep [52]; these animals have Havers canal system, and their oestrous cycle duration is 14–21 days. However, it can be a problem that they are able to spontaneously lose bone volume during the winter because of the decreased bone formation [44]. In the case of a combined model, microstructural bone changes develop over 6 months, as it happened in the case of Lill et al. while they were working with sheep aged 7–9 years. Animals were divided into four groups according to the treatment they had gone through (simulated surgery/ovariectomization/calcium/vitamin D/methylprednisolone). Their BMD was determined every

2 months; then 6 months after the surgeries, the animals were exterminated; and the central located biopsy—taken from vertebrae L3 and L4—was analysed with micro-CT. Results showed that at this species the combined procedure is the most expedient as well, because the ovariectomized, calcium- and vitamin D-withdrawn but methylprednisolone-injected group had the largest BMD, Tb.Th and Tb.N decrease [53].

Neither is the rabbit model common, but Baofeng et al. worked with this model in 2010. Actually, this experiment is very similar to the model of Castaneda et al. [54]. It is a combined model too: osteoporosis was created with the simultaneous ovariectomy and glucocorticoid dosage. BMD in vivo was measured three times, animals were exterminated 10 weeks after the first surgery and the microarchitecture of vertebrae L3 and L4 were examined, as well as mechanical test was run on them. Their outcomes proved that this model is advantageous from many aspects: active Havers remodelling takes place in the bones of the rabbit, this species reaches bone maturity quickly (7–8 months) and besides the time scale of this model is relatively fast (10 weeks) [55].

The advantages of examinations done on dogs are that dogs have Havers canal systems and their intracortical remodelling is the same as the one found in the human's bone system. There are disadvantages to be found as well; judgements of microstructural changes occurring after ovariectomy can vary because dogs only have one oestrous cycle per year [44]. Even so the ovariectomized dog model is useful [56]. Effects of bisphosphates on lumbar vertebra's (L1) spongiosa's microarchitecture and on its changes were tested on female beagles aged 1–2 years. The control group did not receive anything, while the second group received risedronate and the third received alendronate for a year in high concentrate. Micro-CT examinations gave the outcome that microstructure moved towards the plate-like model as a consequence of the treatment and the bone structure became denser compared to the control [57].

Siu et al. worked with a goat model. Averagely aged 3.4-year-old Chinese mountain goats were ovariectomized and then kept on low-calcium diet for 6 months. Important selection criteria were the growth zone's completion of the distal femoralis and the proximal tibia. Both the micro-CT testing and the BMD determination were done on a biopsy of iliac crest at the beginning and then 6 months later. BMD decreased by 16.3% in the 6th month, while BV/TV decreased by 8.34%, Tb.N by 8.51%, Conn.D by 18.52% and Tb.Sp increased by 8.26%. Straightforward positive correlation was determined between BMD and BV/TV, while negative correlation was determined between BMD, Tb.Sp and SMI [58]. Yu et al. did a long-term experiment on Chinese mountain goats. Serum oestrogen levels and the BMD on the vertebrae L1–L4, on the femoral neck and on the diaphysis of femur and tibia were measured at the beginning and 24 months after the ovariectomy and sham surgeries; moreover cyclic mechanic testing was executed on the vertebra, femoral head and femoral neck. Micro-CT examination took place on the vertebra, femoral head and femoral neck only after the extermination. A decrease of the BMD value was found along with a significant decrease of the Tb.N, Tb.Th and BV/TV in the OVX group compared to group SHAM. At the same time, cortical bone porosity was significantly higher at group OVX in the aspect of femoral neck and vertebrae [59].

Osteoporosis experiments conducted on guinea pigs [60] and micropigs might be the rarest [61].

7.3 Micromorphological Changes of Bones in Osteoporosis

Most of the time, it is the first fracture that draws the attention to the fact that someone has osteoporosis. For a long time, the illness lacks any symptoms. However, the broken bones and microfractures accompanied by symptoms are not predominantly derived from the lessened state of the bone tissue; the underlying cause is also the significant change in the microarchitecture

of the bones. These changes occur in the time and the way of appearance bone by bone. Deviations within a certain bone can be found too. For some time besides the changes of the trabecular bone structure, researchers attach increasing importance to the cortical bone loss in the pathogenesis of osteoporosis, especially with patients above the age of 60. Unfortunately, nowadays most anti-osteoporotic drugs used clinically have less effect on cortical bone than trabecular bone, since these two types of bone tissue differ not only in their structure but in their mechanical characteristics and metabolic activity too [62].

When choosing the size of the voxel, we have to consider that a too high resolution expands the time of scanning and makes it harder to manage the file. The voxel number at the same time must be high enough in order to manage to catch the complex structure of the bone. It seems that it is enough if six voxels form one trabecula along the thickness direction to analyse the structure, and for the acceptable accurateness of the finite element analysis (FEA) model, it is also appropriate if six elements create a trabecula [63].

When setting the value of the threshold, we create a binary picture from a complex picture. It is a qualitative definition, if a calibrated expert compares the original greyscale images to the picture of the segmented trabecular bone. It is quantitative, if it is determined based on a histogram what counts as bone tissue and what does not. In the case of the global threshold, there is a set threshold for the whole data set, while by the local threshold, there is a different threshold value assigned to each and every pixel, based on the greyscale information of the adjacent pixels [64].

In the research done by Isaksson et al., the standardized sampling was taken from alive subjects' iliac crest area, cadavers, femur and the tibia's condylus medialis or the medialis plateau. The donors were males and females, alive and cadaver, who were divided into groups: osteoporotic and ones with normal bones based on DXA, clinical diagnosis and quantitative histomorphometrics. The size of the voxel was 14 μm at the iliac samples and 18 μm by the femur and the tibia. Two different threshold techniques were used in every case, global threshold independently from the size of the voxel and local threshold used with a technique demonstrated by Waarsing [65]. Taken everything into consideration, they found that the algorithm using local thresholds is less applicable, when we want to show the difference between the highlighted parameters (BV/TV, Tb.Th, Tb.Sp, DA, SMI), and that the value of BV/TV does not change significantly in normal bone structure over 150 micron voxel size, but by osteoporotic samples deviation can be seen, even in the case of a smaller voxel size [66].

Longo et al.'s experiment draws special attention to choosing the right voxel size. They analysed the rat tibias, using micro-CT on an ovariectomized model, with an in vivo 18 μm and ex vivo 9 and 18 μm resolution. There was no difference by 18 micron voxel size between the in vivo and ex vivo scanning in the analysed bone parameters. However when comparing the values obtained using 9 micron voxel size to the ones obtained using 18 micron voxel size, Conn.D is significantly lower, and Tb.Th and the Ct.Th are significantly higher at 18 micron resolution both by OVX and SHAM groups, although most of the parameters are correlated with the parameters obtained using 9 micron ex vivo scan settings [67].

In a research conducted on a vertebra belonging to a mouse, the pixel size was varied between 6 and 30 micron, and the threshold values were defined both quantitatively and qualitatively. They found that certain parameters are highly depending on the voxel size, for example, CD and Tb.Th, but with other parameters like Tb.N and Tb.Sp, there was no significant difference either by small or bigger voxel size. By small voxel size, the two threshold techniques concluded in similar results, but when increasing the voxel size, the differences were increasing. The qualitative segmenting technique was more effective for measuring BV/TV and Tb.Th besides varying voxel sizes, while the quantitative technique seemed to be more effective in the case of Tb.N, Tb.Sp and SMI [68].

Milovanovic et al. found in his research that when examining the femoral neck cortical of both healthy women and women with osteoporosis and contralateral hip fracture, the fragile bone demonstrated lower pore volume at the measured scales. The investigated pore size was between 7.5 and 1500 nm. In the healthy bone 200 to

1500 nm pores were present in a higher rate. The osteoporotic bone is known for increased porosity at macroscopic level and level of tens or hundreds of microns, but this study with a unique assessment range of nano- to micron-sized pores reveals that osteoporosis does not imply increased porosity at all length scales [69].

7.3.1 Micromorphological Changes in Vertebra

The prevalence of broken vertebra is higher in younger generations than any osteoporotic fractures, i.e. hip fractures. The annual occurrence of osteopathic vertebrae fractions can be hardly determined, because a substantial proportion of the fractures remains unrecognized in clinical practice. But whether they cause complaints or not, a broken vertebra causes increased morbidity and mortality [70]. When testing on humans [71], rats [27], mice [38] and on other species [48, 53] inside the vertebral body, we usually see the following changes while performing micro-CT analysis: the trabeculae are getting thinner, they are mostly rod forms, the distance between them is increasing and the BV/TV connectivity decreases [71].

7.3.2 Micromorphological Changes in the Femur and Tibia

The distal femur and proximal tibia are the most investigated fields of the osteoporosis research done by micro-CT, usually in animal testing. A well-defined and assessable-sized region of interest (ROI) can be marked out even in the case of the mouse. Marking out the ROI in the case of meta- and diaphysis spongiosa and cortical research can be conducted easily by keeping a certain distance from the growth plate. Femoral neck is a rarely investigated area with micro-CT [69], although it is used in more models conducting mechanical tests [72]. While examining humans in this area in the spongiosa, even aging results in a 20% decrease in BV/TV and Tb. Th, Conn.D and Tb.N also decrease in both genders [73]. It was observed on more occasions that osteoporotic microstructure changes can be detected earlier in the trabecular bone structure of the vertebra than in the spongiosa of the femur and the tibia [20, 38]. In osteoporosis by these bones, mainly BMD decrease was observed along with a decrease in BV/TV, Tb.Th and Tb.N and rod-form trabeculae [39, 74] (Fig. 7.4).

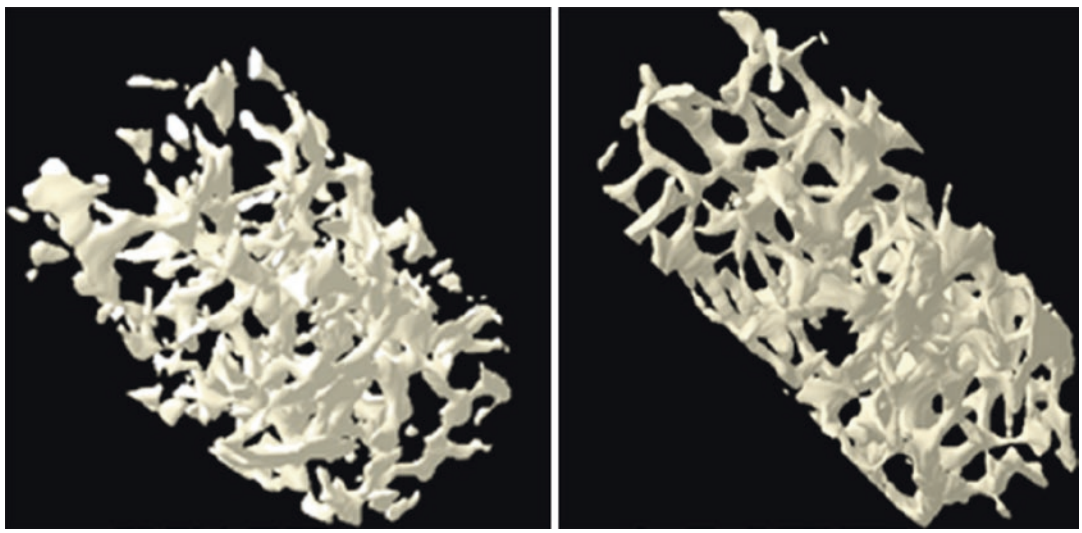

Fig. 7.4 OVX and SHAM trabecular bone from mouse tibia

7.3.3 Micromorphological Changes in the Mandible and Maxilla

In a systematic review, published in 2015, attention is drawn to the fact that the examination areas of the rodents' jaw microstructure are rather heterogenic and standardization would be required [75]. Most frequently on the maxilla, the alveolar bone around the first molars, the interradicular septum is examined. On the mandible, the alveolar bone around the molars, the area between the molars and the incisor and the base of the mandible are determined differently by each author, and the condylus are investigated [75]. Defining the ROI is a more difficult task in this case, harder than with the other bones, mainly because of the small size of the sample (Fig. 7.5).

The examination of alveolar bone structure in osteoporosis shows a different result: in some cases, no significant changes were found in these areas [32], or at least slower-evolving and less significant changes were found in the bone structure [45], but in other cases, damage of the bone tissue similar to those found in other bones was found, correlated with the bone marker molecules [7].

In the condylus of the mandible, two regions, the anterior and posterior, were examined on an ovariectomized rat model by Tanaka et al. The anterior and the posterior regions showed different bone dynamics. In the OVX group, the bone volume (BV) decreased significantly in the posterior area, though there was no change in the anterior. At the same time in the anterior region, BV was increasing while aging in the SHAM group, and there was no change found in the posterior area. An explanation for this deviation might be that the mechanical stress caused by occlusion affects the two regions differently. The tendency of decreasing bone mass caused by oestrogen deficiency was to be seen in both regions, with time passing by [76].

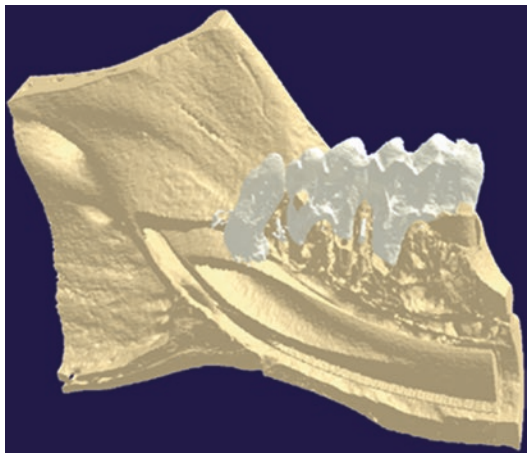

Fig. 7.5 The most commonly used ROIs on mandible are between the roots of molars

7.3.4 Future Trends in Analysis of Micromorphological Changes of Cancellous Bone in Osteoporosis

As can be seen from the above, micro-CT is a widespread method for the analysis of the microstructure of the spongiosa, in the case of samples of both human and of animal origin. Data derived this way, or data calculated from these, describe the current state of the trabecular bone structure well. For analysing bone stiffness and locating the potential area, where a bone fracture might occur, a numerical method is used, called finite element analysis (FEA)[77], which has been more and more widely used in biomechanics since 1972 [78]. There is an increasing number of algorithms based on the data of the micro-CT to simulate bone remodelling [79]. Wu et al. tried to find an approach based on micro-CT data to evaluate the changes in bone structure and determine the bone stiffness as quickly as possible especially in the case of longitudinal in vivo examinations [63]. A new field of usage is the mechanical testing of the 3D printed trabecular bone structure, created from micro-CT data. In Barak et al.'s research in the case of the chimpanzee third metacarpal head, they found that an 8% BT/TV decrease results in a 17% structural stiffness and a 24% structural strength decrease [80]. The key step of this analysis is to choose a threshold method and a resolution correctly.

7.3.5 Micromorphological Changes of Cortical Bone in Osteoporosis

When examining the structure of the corticalis, for quite some time, the histological examination was the gold standard. Therefore they wished to compare micro-CT and histological results on human tibia and femur samples. They used two threshold values during the segmentation: one higher than that scanned from the air and the other lower than the sample embedded into the PMMA. Cortical porosity (Ct.Po), canal separation (Ca.Sp) and canal diameter (Ca.Dm) data measured on both histological and micro-CT showed good correspondence and good correlation. It was also revealed that if the threshold value is adequate, then the medium surrounding the sample has no influence on the results [81] (Fig. 7.6).

The cortical of bones gets slimmer while aging, even without the presence of osteoporosis. Tiede-Lewis et al. examined the changes in the cortical bone on a mouse model. In their experiment they compared the femur of 5-month-old and 22-month-old C57BL/6 mice. The analysis of the microstructure with the help of micro-CT was conducted on both male and female mice, they analysed the microstructure with micro-CT and they found that in the area of the distal femur, the cortical BV/TV decreased by 6.3% in female mice, while in males it decreased only by 19%. By these significant changes, not only there is a decreasing number of dendrite in the osteocytes, but the cell density is reduced too. The decrease in dendricity precedes the decrease in the number of osteocytes, giving the impression that the prior is a trigger of the reduced vitality of the osteocytes. However, the osteocytes have a key role of maintaining bone volume [82].

While examining the cortical in the case of a rabbit's femur by Pazzaglia et al., micro-CT pictures were used to calculate tissue volume (TV), canal volume (CaV), Ct.Po and canal surface (CS). Subperiosteally higher canal number was found then subendosteally [83]. In the case of rats, Kim JN et al., in an aforementioned research, found wider diameter and higher connectivity Havers canals near the endosteal area, than subperiosteally [23].

Cortical canals can be visualized on the rat tibia on micro-CT slices and can also be used to examine percent porosity and mean canal diameter with global thresholding [84].

7.4 Materials and Methods of Our Mice Study

While the negative effects of osteoporosis on the quality of the bone and the increased risk of fracture in the vertebrae and long bones are well known and frequently tested in experiments,

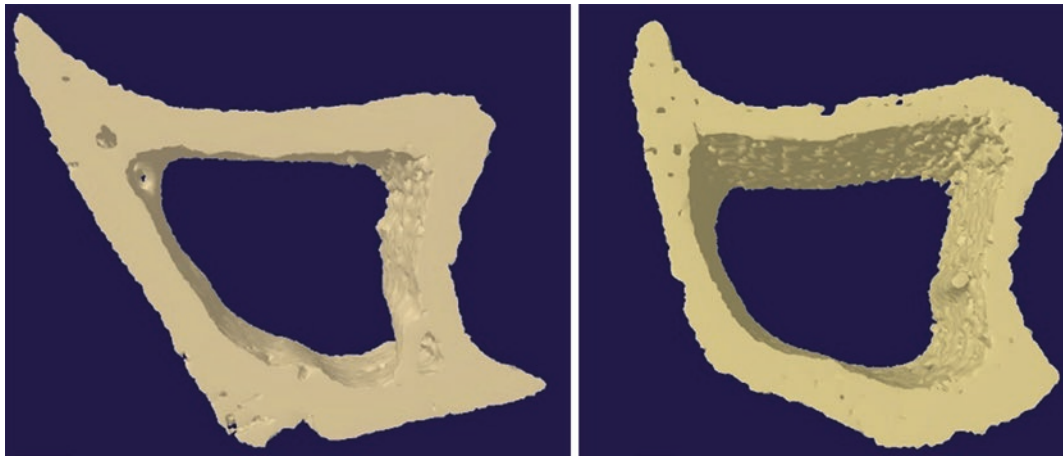

Fig. 7.6 SHAM and OVX cortical bone from mouse tibia

changes in the jaw are less clear. The structure of the mandible and maxilla due to their function and unlike other bones and, uniquely, because of the teeth that are fixed in them, is even more complex. Experiments have shown that postmenopausal osteoporosis can play a role in the progression of periodontal disease and consequent tooth loss [85, 86] but also in later alveolar wound healing [87]. Still, the involvement of the jaw bone in osteoporosis, perhaps because of the different sampling sites, is disputed. Our aim was to investigate the changes in the trabecular and cortical bone structure of the mandible and the femur together while adding vitamin D on the OVX mouse model.

7.4.1 Examination of Femur and Mandible

We divided 30 6-week 22 g CRL:OF1 (Charles River Laboratories) mice into three groups. Ten members of the D3 group after ovariectomy had received vitamin D each day for 6 weeks (4 ng/day, Alpha D3-TEVA 0.25 μg), while ten members of the OVX group after the operation, and ten members of the SHAM group after the sham operation during the period of examination received peanut oil as a vehicle. Following the extermination of the animals, the left hemimandibulas and the left femur were removed and stored in phosphate-buffered saline containing 0.02% sodium aside at 4 degrees Celsius. Scanning was done by Skyscan 1172 (Bruker, Kontich, Belgium). For femur the scanning protocol was set at X-ray energy settings of 50 kV and 198 μA, and the voxel size was 5.02 μm. The settings for the mandible were 70 kV, 114 μA and 7.1 μm. In both cases 0.5 mm Al-filter and 0.5 degree rotation degree were used. The reconstruction was performed with the NRECON (Skyscan, Burker) software; the analysis of the microarchitecture of the mandible and the femur was implemented with the CT Analyzer 1.7.0.0 (Skyscan, Burker) software. During the segmentation global manual threshold technique was applied. For the examination of the parameters of the mandibula spongiosa, we used the area between the roots of the first molar tooth. The attributes of the mandibula corticalis were examined at the base of the mandible starting from the distal surface of the root of the third molar through 250 mesial slices (Fig. 7.7).

Femurine ROI was determined from the growth plate at the distal epiphysis. From here, the parameters of the trabecular bone were analysed in 400 slices (1.807 mm) from the height of 50 slices measured in the direction of diaphysis. We specified the examination of the cortical bone between the 500. and 600. slices counted from the growth plate (Fig. 7.8).

Statistical analysis was performed using SPSS 24.0 (SPSS, Chicago, IL, USA) software. Kruskal-Wallis test was applied. Significance was set at $p < 0.05$. Then Tukey's post hoc test was used.

7.4.2 Results

In the cortical bone of the femur, Ct.Th was significantly lower in the OVX group than in SHAM or D3 ($p < 0.005$) (Fig. 7.9). There were no significant changes in mandibular cortical bone in the examined parameters.

In the trabecular bone of the femur, BV/TV was significantly lower in the OVX group than in SHAM ($p < 0.001$), Tb.Th was significantly lower in the OVX group compared to SHAM and D3 ($p < 0.05$), and Tb.Pf in the OVX group was significantly higher than in the SHAM group ($p < 0.005$). BS/BV was higher in the OVX group compared to D3 and SHAM ($p = 0.064$). In this case, an increase in the number of elements would be required to confirm any significance (Fig. 7.10).

In trabecular bone of the mandible in the OVX group, BV/TV was significantly lower than in the SHAM or D3 group ($p < 0.05$), BS/BV in the OVX group was significantly higher than in the SHAM group ($p < 0.05$) and Tb.Th in the OVX group was significantly lower than in SHAM or D3 ($p < 0.005$) (Fig. 7.11).

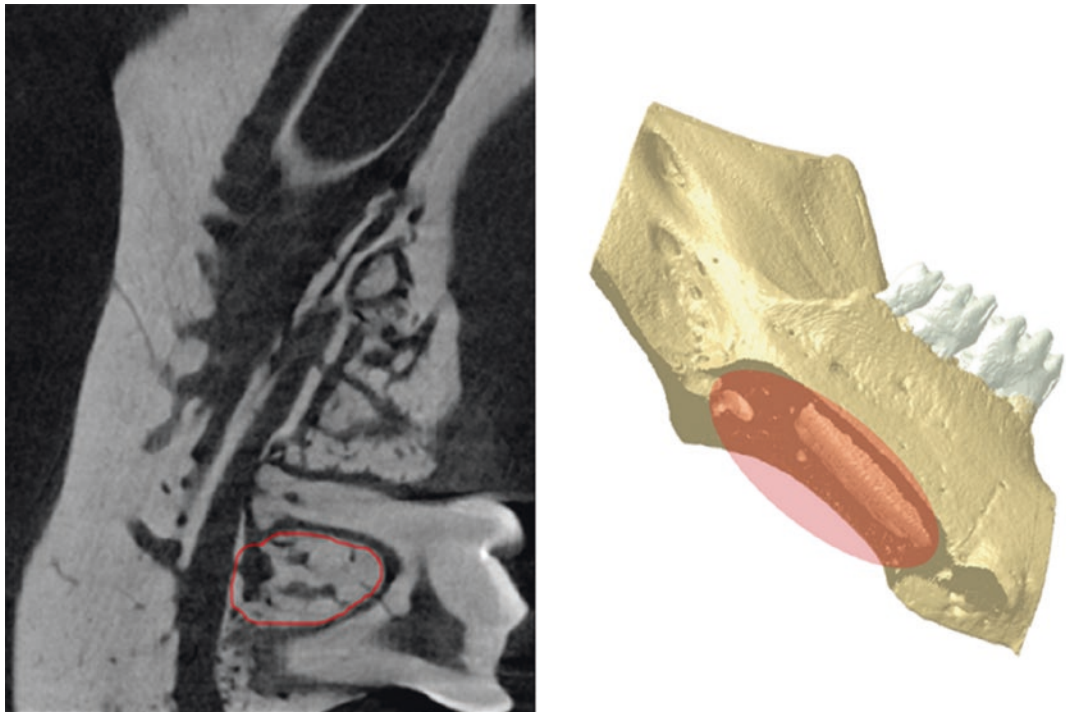

Fig. 7.7 Mandibular ROIs

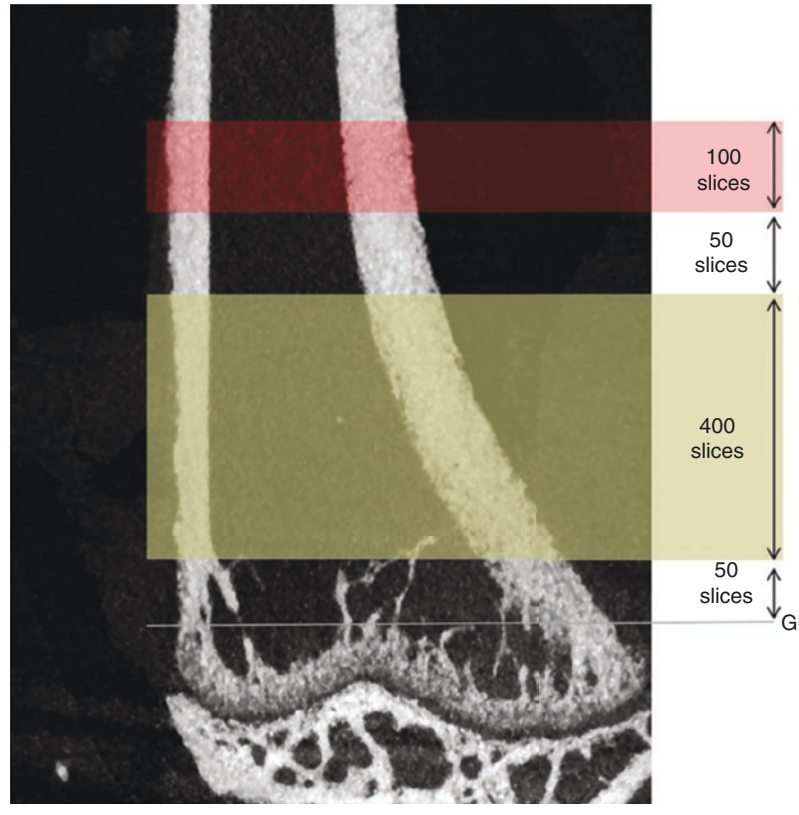

Fig. 7.8 ROIs from femur

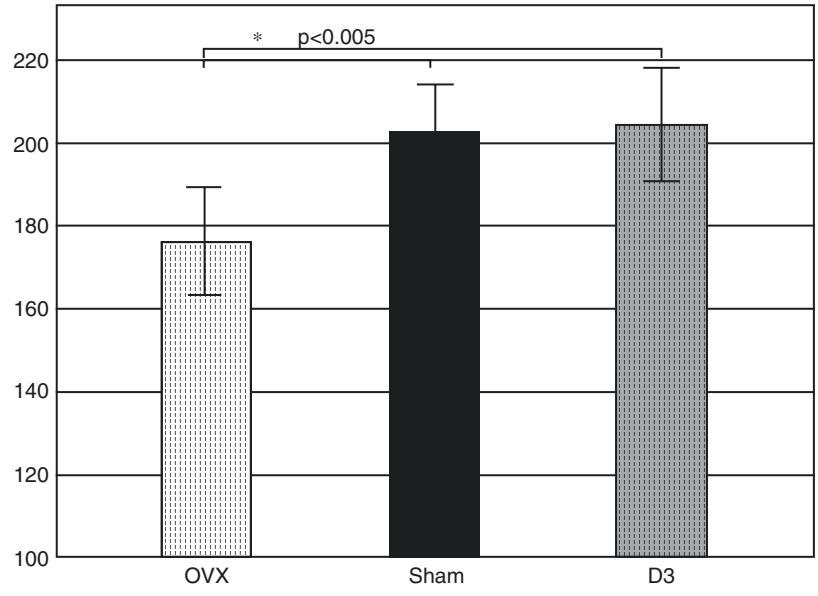

Fig. 7.9 The cortical thickness in femur ($n = 10$)

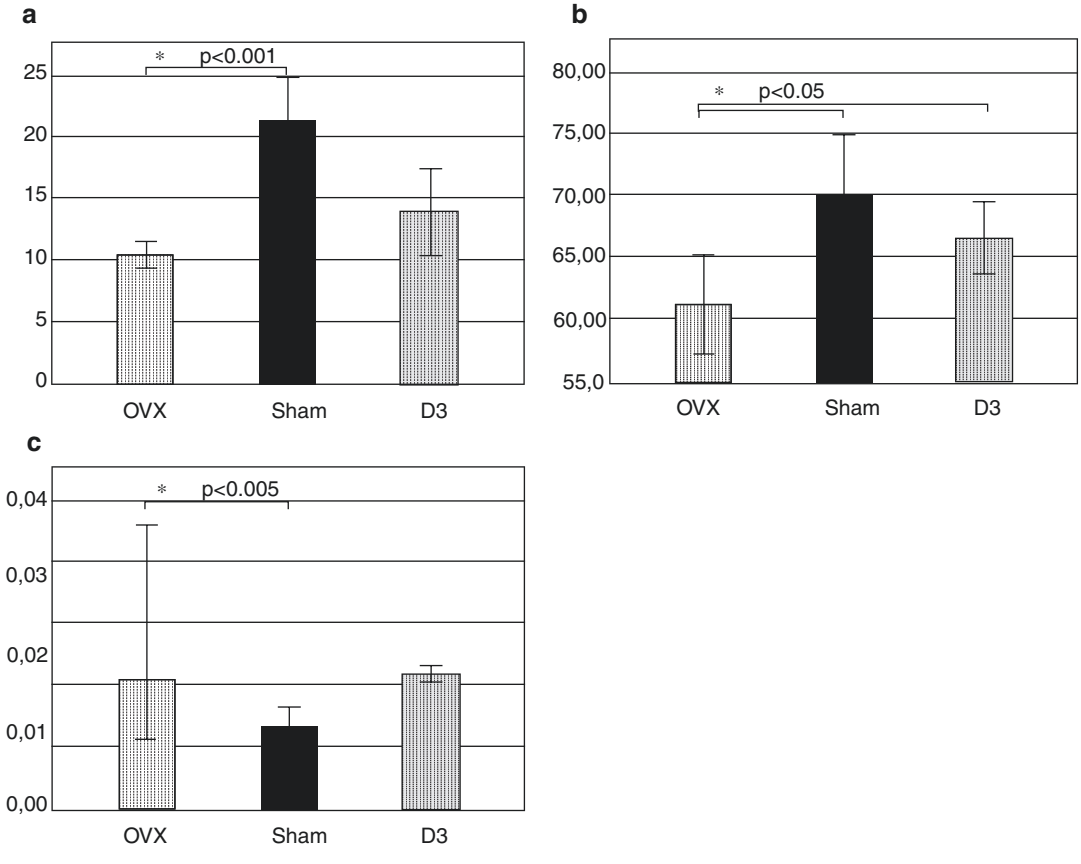

Fig. 7.10 Micromorphological results in trabecular bone of the femur. (**a**) BV/TV; (**b**) Tb.Th; (**c**); Tb.Pf ($n = 10$)

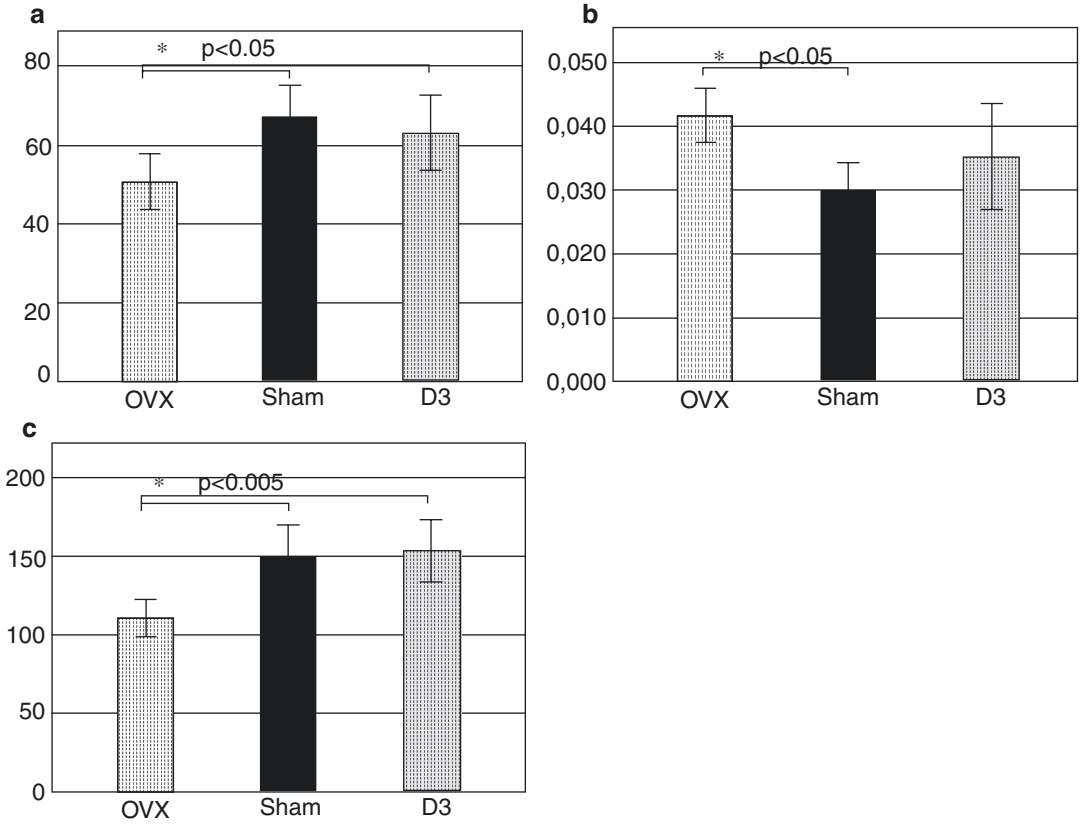

Fig. 7.11 Micromorphological results in trabecular bone of the mandible. (**a**) BV/TV; (**b**) BS/BV (**c**) Tb.Th (n = 10)

7.4.3 Discussion

In the cortical examination, the results showed that in the OVX group, femoral cortical bone tends to become thinner due to oestrogen deficiency, and this negative change could be eliminated by the administration of vitamin D3. In contrast, there was no significant change in the cortical mandible. Considering the tendency of the data, this may be due to the need for more time to change the cortical thickness of the mandible than for long bones. Lee et al. investigated the development of renal osteodystrophy on mouse mandible, and at the end of week 15, the cortical was significantly thinner [88]. In a surgical model of postmenopausal osteoporosis in chronic kidney disease (CKD), in the case of mouse, 12 weeks after ovariectomy, mandibular cortical thickness was significantly lower in OVX and OVX + CDK groups compared to SHAM in Guo et al.'s study [89].

The bone parameter determinations in trabecular bone both in the case of femur and mandible also resulted in significantly lower BV/TV values in the OVX group compared to SHAM and D3 groups. Likewise, BV/TV was also lower in both study areas in the OVX group for SHAM and for mandible in relation to D3. The increase in BS/BV values in the OVX group, consistent with the previous parameters, shows a weakened microarchitecture in both bones in the OVX group. Based on the results of the D3 group, it can be said that in both designated test areas, microstructural damage to bone tissue was reduced. The assessment of alveolar bone involvement in osteoporosis is controversial in the literature. Sheng et al. found that the bone structure of the mandibula was less responsive to the osteoprotegerin (OPG)

gene deprivation than the tibia [42]. In the study of Bouvard et al., the BV/TV value of alveolar bone decreased significantly in 28 days [41]. Ejiri et al. examining the alveolar bone structure on OVX rat model found that serious bone loss was caused by high bone resorptive activity, which was accelerated immediately after ovariectomy, followed by a milder, but longer-lasting, resorptive activity. During this time, trabecules are separated into smaller fragments, while their number decreases, so their recovery is very cumbersome [87]. In their examinations, it was concluded that occlusal hypofunction could significantly increase the fragility of the bone structure around the teeth [87]. The cause of the mentioned controversy may be different ROI. Johnston et al. call attention in that the alveolar bone ROI should be limited to the interradicular septum of the first molar, because it is the most well-characterized site and appears to respond positively to the established bone-sparing effect of oestrogen [90].

7.5 Summary

In our study the microstructure of mandibular and femoral trabecular bone changed in the same way under the influence of ovariectomy in 6 weeks, and the protective effects of vitamin D were also shown in the two test sites. To observe the changes of cortical bone in the case of the mandible, 6 weeks were not enough, unlike in the case of the femur.

References

1. Nieves JW, Formica C, Ruffing J, Zion M, Garrett P, Lindsay R, Cosman F. Males have larger skeletal size and bone mass than females, despite comparable body size. J Bone Miner Res. 2005;20:529–35.
2. Barling PM. Osteoporosis - an increasingly important issue for both young and aging citizens of Malaysia. leJSME. 2013;7(1):1–3.
3. Eckstein F, Matsuura M, Kuhn V, Priemel M, Müller R, Link TM, Lochmüller EM. Sex differences of human trabecular bone microstructure in aging are site-dependent. J Bone Miner Res. 2007;22:817–24.
4. Dufresne TE, Chmielewski PA, Manhart MD, Johnson TD, Borah B. Risedronate preserves bone architecture in early postmenopausal women in 1 year as measured by three-dimensional microcomputed tomography. Calcif Tissue Int. 2003;73:423–32.
5. Arlot ME, Jiang Y, Geneant HK. Histomorphometric and microCT analysis of bone biopsie from postmenopausal osteoporotic women treated with strontium ranelate. J Bone Miner Res. 2008;23:215–22.
6. Fox J, Miller MA, Recker RR, Sp B, Smith SY, Moreau I. Treatment of postmenopausal osteoporotic women with parathyroid hormone 1-84 for 18 months increases cancellous bone formation and improves cancellous architecture: a study of iliac crest biopsy using histomorphometry and micro computed tomography. J Musculoskelet Neuronal Interact. 2005;5:356–7.
7. Yamashita-Mikami E, Tanaka M, Sakurai N, Arai Y, Matsuo A, Ohshima H, Nomura S, Ejiri S. Correlation between alveolar bone microstructure and bone turnover marker sin pre- and post-menopausal women. Oral Maxillofac Surg. 2013;115:12–9.
8. Thompson DD, Simmons HA, Pirie CM, Ke HZ. FDA guidelines and animal models for osteoporosis. Bone. 1995;17(4 Suppl):125–33.
9. Gallagher A, Chambers TJ, Tobias JH. The estrogen antagonist ICI 182,780 reduces cancellous bone volume in female rats. Endocrinology. 1993;133:2787–91.
10. Goulding A, Gold E. A new way to induce oestrogen-deficiency osteopaenia in the rat: comparison of the effects of surgical ovariectomy and administration of the LHRH agonist buserelin on bone resorption and composition. J Endocrinol. 1989;121:293–8.
11. Zeng QQ, Jee WS, Bigornia AE, King JG Jr, D'Souza SM, Li XJ, Ma YF, Wechter WJ. Time responses of cancellous and cortical bones to sciatic neurectomy in growing female rats. Bone. 1996;19:13–21.
12. Thompson DD, Rodan GA. Indomethacin inhibition of tenotomy-induced bone resorption in rats. J Bone Miner Res. 1988;3:409–14.
13. Tian XY, Jee WS, Li X, Paszty C, Ke HZ. Sclerostin antibody increases bone mass by stimulating bone formation and inhibiting bone resorption in a hindlimb-immobilization rat model. Bone. 2011; 48(2):197–201.
14. Kim C, Park D. The effect of restriction of dietary calcium on trabecular and cortical bone mineral density in the rats. J Exerc Nutr Biochem. 2013;17(4):123–31.
15. Lelovas PP, Xanthos TT, Thoma SE, Lyritis GP, Dontas IA. The laboratory rat as an animal model for osteoporosis research. Comp Med. 2008;58:425–30.
16. Frost HM, Jee WSS. On the rat model of human osteopenias and osteoporoses. Bone Miner. 1992;18:227–36.
17. Khajuria DK, Razdan R, Mahapatra DR. Description of a new method of ovariectomy in female rats. Rev Bras Reumatol. 2012;52(3):462–70.
18. Gao X, Ma W, Dong H, Yong Z, Su R. Establishing a rapid animal model of osteoporosis with ovariectomy plus low calcium diet in rats. Int J Clin Exp Pathol. 2014;7(8):5123–8.

19. Dennison E, Cole Z, Cooper C. Diagnosis and epidemiology of osteoporosis. Curr Opin Reumatol. 2005;17:456–61.
20. Jee WS, Yao W. Overview: animal models of osteopenia and osteoporosis. J Musculoskelet Neuronal Interact. 2001;1(3):193–207.
21. Egermann M, Goldhahn J, Schneider E. Animal models for fracture treatment in osteoporosis. Osteoporos Int. 2005;16:129–38.
22. Turner RT, Maran A, Lotinun S, Hefferan T, Evans GL, Zhang M, Sibonga JD. Animal models for osteoporosis. Rev Endocr Metab Disord. 2001;2:117–27.
23. Kim JN, Lee JY, Shin KJ, Gil YC, Koh KS, Song WC. Haversian system of compact bone and comparison between endosteal and periosteal sides using three-dimensional reconstruction in rat. Anat Cell Biol. 2015;48(4):258–61.
24. Brouwers JEM, van Rietbergen B, Huiskes R, Ito K. Effects of PTH treatment on tibia bone of ovariectomized rats assessed by in vivo micro-CT. Osteoporos Int. 2009;20(11):1823–35.
25. Iwaniec UT, Moore K, Rivera MF, Myers SE, Vanegas SM, Wronski TJ. A comparative study of the bone-restorative efficacy of anabolic agents in aged ovariectomized rats. Osteoporos Int. 2007;18(3):351–62.
26. Dai QG, Zhang P, Wu YQ, Ma XH, Pang J, Jiang LY, Fang B. Ovariectomy induced osteoporosis in the maxillary alveolar bone: an in vivo micro-CT and histomorphometric analysis in rats. Oral Dis. 2014;20(5):514–20.
27. Yoon KH, Cho DC, Yu SH, Kim KT, Jeon Y, Sung JK. The change of bone metabolism in ovariectomized rats: analyses of microCT scan and biochemical markers of bone turnover. J Korean Neurosurg Soc. 2012;51(6):323–7.
28. Sharma D, Larriera AI, Palcio-Mancheno PE, Gatti V, Fritton JC, Bromage TG, Cardoso L, Doty SB, Fritton SP. The effects of estrogen deficiency on cortical bone microporosity and mineralization. Bone. 2018;110:1–10.
29. Ames MS, Hong S, Lee HR, Fields HW, Johnston WM, Kim DG. Estrogen deficiency increases variability of tissue mineral density of alveolar bone surrounding teeth. Arch Oral Biol. 2010;55(8):599–605.
30. Yang J, Farnell D, Devlin H, Horner K, Graham J. The effect of ovariectomy on mandibular cortical thickness in the rat. J Dent. 2005;33(2):123–9.
31. Mavropoulos A, Rizzoli R, Ammann P. Different responsiveness of alveolar and tibial bone to bone loss stimuli. J Bone Miner Res. 2007;22(3):403–10.
32. Kozai Y, Kawamata R, Sakurai T, Kanno M, Kashima I. Influence of prednisolone-induced osteoporosis on bone mass and bone quality of the mandible in rats. Dentomaxillofacial Radiol. 2009;38(1):34–41.
33. Blazsek J, Dobó-Nagy CS, Blazsek I, Varga R, Vecsei B, Fejérdy P, Varga G. Aminobisphosphonate stimulates bone regeneration and enforces consolidation of titanium implant into a new rat caudal vertebra model. Pathol Oncol Res. 2009;15:567–77.
34. Bain SD, Bailey SC, Celino DL, Lantry MM, Edwards MW. High-dose estrogen inhibits bone resorption and stimulates bone formation in the ovariectomized mouse. J Bone Miner Res. 1993;8:435–42.
35. Ferguson VL, Ayers RA, Bateman TA, Simske SJ. Bone development and age-related bone loss in male C57BL/6J mice. Bone. 2003;33:387–98.
36. Glatt V, Canalis E, Stadmeyer L, Bouxsein ML. Age-related changes in trabecular architecture differ in female and male C57BL/6J mice. J Bone Miner Res. 2007;8:1197–207.
37. Willinghamm MD, Brodt MD, Lee KL, Stephens AL, Ye J, Silva MJ. Age-related changes in bone structure and strength in female and male BALB/c mice. Calcif Tissue Int. 2010;86(6):470–83.
38. Chen H, Zhou X, Emura S, Shoumura S. Site-specific bone loss in senescence-accelerated mouse (SAMP6): a murine model for senile osteoporosis. Exp Gerontol. 2009;44(12):792–8.
39. Cano A, Dapía S, Noguera I, Pineda B, Hermenegildo C, del Var R, Caeiro JR, García-Pérez MA. Comparative effects of 17 B-estradiol, raloxifene and genistein on bone 3D microarchitecture and volumetric bone mineral density in the ovariectomized mice. Osteoporos Int. 2008;19(6):793–800.
40. Willey JS, Livingston EW, Robbins ME, Bourland JD, Tirado-Lee L, Smith-Sielicki H, Bateman TA. Risedronate prevents early radiation-induced osteoporosis in mice at multiple skeletal location. Bone. 2010;46(1):101–11.
41. Bouvard B, Gallois Y, Legrand E, Audran M, Chappard D. Glucocorticoids reduce alveolar and trabecular bone in mice. Joint Bone Spine. 2013;80(1):77–81.
42. Sheng ZF, Xu K, Ma YL, Liu JH, Dai RC, Zhang YH, Jiang YB, Liao EY. Zoledronate reverses mandibular bone loss in osteoprotegerin-deficient mice. Osteoporos Int. 2009;20(1):151–9.
43. He XY, Zhang G, Pan XH, Liu Z, Zheng LZ, Chan CW, Lee KM, Cao YP, Li G, Wei L, Hung LK, Leung KS, Qin L. Impaired bone healing pattern in mice with ovariectomy-induced osteoporosis: a drill-hole defect model. Bone. 2011;48(6):1388–400.
44. Bonucci E, Ballanti P. Osteoporosis-bone remodeling and animal models. Toxicol Pathol. 2014;42(6):957–69.
45. Binte Anwar R, Tanaka M, Kohno S, Ikegame M, Watanabe N, Nowazesh Ali M, Ejiri S. Relationship between porotic changes in alveolar bone and spinal osteoporosis. J Dent Res. 2007;86:52–7.
46. Ominsky MS, Boyd SK, Varela A, Jolette J, Felx M, Doyle N, Mellal N, Smith SY, Locher K, Buntich S, Pyrah I, Boyce RW. Romosozumab improves bone mass and strength while maintaining bone quality in ovariectomized cynomolgus monkeys. J Bone Miner Res. 2017;32(4):788–801.
47. Cabal A, Williams DS, Jayakar RY, Zhang J, Sardesai S, Doung LT. Long-term treatment with odanacatib maintains normal trabecular biomechanical properties in ovariectomized adult monkeys as demonstrated by

micro-CT based finite element analysis. Bone Rep. 2017;6:26–33.
48. Hordon LD, Itoda M, Shore PA, Heald M, Brown M, Kanis JA, Rodan GA, Aaron JE. Preservation of thoracic spine microarchitecture by alendronate: comparison of histology and microCT. Bone. 2006;38:444–9.
49. Borah B, Dufresne TE, Cockman MD, Gross GJ, Sod EW, Myers WR, Combs KS, Higgins RE, Pierce SA, Stevens ML. Evaluation of changes in trabecular bone architecture and mechanical properties of minipig vertebrae by three-dimensional magnetic resonance microimaging and finite element modeling. J Bone Miner Res. 2000;15(9):1786–97.
50. Pautke C, Kreutzer K, Weitz J, Knödler M, Münzel D, Wexel G, Otto S, Hapfelmeier A, Stürzenbaum S, Tischer T. Bisposphonate related osteonecrosis of the jaw: a minipig large animal model. Bone. 2012;51(3):592–9.
51. Tsutsumi H, Ikeda S, Nkamura T. Osteoporosis model in minipigs. In: McAnulty PA, Dayan AD, Ganderup NC, Hastings KL, editors. The minipig in biomedical research. Boca Raton, FL: CRC Press; 2012. p. 517–25.
52. Chavassieux P, Garnero P, Duboeuf F, Vergnaud P, Brunner-Ferber F, Delmas PD, Meunier P. Effects of a new selective estrogen receptor modulator (MDL 103,323) on cancellous and cortical bone in ovariectomized ewes: a biochemical, histomorphometric, and densitometric study. J Bone Miner Res. 2001;16(1):89–96.
53. Lill CA, Fluegel AK, Schneider E. Effect of ovariectomy, malnutrition and glucocorticoid application on bone properties in sheep: a pilot study. Osteoporos Int. 2002;13(6):480–6.
54. Castaneda S, Calvo E, Largo R, Gonzalez-Gonzalez R, de La Piedre C, Diaz-Curiel M, Herrero-Beaumont G. Characterization of a new experimental model of osteoporosis in rabbits. J Bone Miner Metab. 2008;26(1):53–9.
55. Baofeng L, Zhi Y, Bei C, Guolin M, Quingshui Y, Jian L. Characterization of a rabbit osteoporosis model induced by ovariectomy and glucocorticoid. Acta Orthop. 2010;81(3):396–401.
56. Wilson AK, Bhattacharyya MH, Miller S, Mani A, Sacco-Gibson N. Ovariectomy-induced changes in aged beagles: histomorphometry of rib cortical bone. Calcif Tissue Int. 1998;62(3):237–43.
57. Ding M, Day JS, Burr DB, Mashiba T, Hirano T, Weinans H, Sumner DR, Hvid I. Canine cancellous bone microarchitecture after one year of high-dose bisphosphonates. Calcif Tissue Int. 2003;72(6):737–44.
58. Siu WS, Qin L, Cheung WH, Leung KS. A study of trabecular bones in ovariectomized goats with micro-computed tomography and peripheral quantitative computed tomography. Bone. 2004;35(1):21–6.
59. Yu Z, Wang G, Tang T, Fu L, Yu X, Zhu Z, Dai K. Long-term effects of ovariectomy on the properties of bone in goats. Exp Ther Med. 2015;9(5):1967–73.
60. Ding M, Danielsen CC, Hvid I. The effects of bone remodeling inhibition by alendronate on three-dimensional microarchitecture of subchondral bone tissues in guinea pig primary osteoarthrosis. Calcif Tissue Int. 2008;82(1):77–86.
61. Kim SW, Kim KS, Solis CD, Lee MS, Hyun BH. Development of osteoporosis animal model using micropigs. Lab Anim Res. 2013;29(3):174–7.
62. Li J, Bao Q, Chen S, Liu H, Feng J, Qin H, Liu D, Shen Y, Zhao Y, Zong Z. Different bone remodeling levels of trabecular and cortical bone in response to changes in Wnt/B-catenin signaling in mice. J Orthop Res. 2017;35(4):812–9.
63. Wu Y, Adeeb S, Doschak MR. Using micro-CT derived bone microarchitecture to analyze bone stiffness—a case study on osteoporosis rat bone. Front Endocrinol. 2015;6:1–7.
64. Firdousi R, Parveen S. Local threshold techniques in image binarization. Int J Engin Comput Sci. 2014;3(3):4062–5.
65. Waarsing JH, Day JS, Weinans H. An improved segmentation method for in vivo microCT imaging. J Bone Miner Res. 2004;19(10):1640–50.
66. Isaksson H, Töyräs J, Hakulinen M, Aula AS, Tamminen I, Julkunen P, Kröger H, Jurvelin JS. Structural parameters of normal and osteoporotic human trabecular bone are affected differently by microCT images resolution. Osteoporos Int. 2011;22(1):167–77.
67. Longo AB, Salomon PL, Ward WE. Comparison of ex vivo and in vivo micro-computed tomography of rat tibia at different scanning settings. J Orthop Res. 2017;35(8):1690–8.
68. Christiansen BA. Effect of micro-computed tomography voxel size and segmentation method on trabecular bone microstructure measures in mice. Bone Rep. 2016;5:136–40.
69. Milovanovic P, Vukovic Z, Antonijevic DD, Zivkovic V, Nikolic S, Djuric M. Porotic paradoxon: distribution of cortical bone sizes at nano- and micro-levels in healthy vs. fragile human bone. J Mater Sci Mater Med. 2017;28(5):71–7.
70. Oszteoporotikus csigolyatörések I. rész 2007 Oszteológiai Közlemények 3:137–146.
71. Cesar R, Boffa RS, Fachine LT, LeviasTP SAMH, Pereira CAM, Reiff RBM, Rollo JMDA. Evaluation of trabecular microarchitecture of normal osteoporotic and osteopenic human vertebrae. Proc Engineer. 2013;59:6–15.
72. Mackay DL, Kean TJ, Bernardi KG, Haeberle HS, Ambrose CG, Lin F, Dennis JE. Reduced bone loss in a murine model of postmenopausal osteoporosis lacking complement component 3. J Orthop Res. 2018;36(1):118–28.
73. Chen H, Zhou S, Shoumura S, Emura S, Bunai Y. Age- and gender-dependent changes in three-dimensional microstructure of cortical and trabecular bone at the human femoral neck. Osteoporos Int. 2010;21(4):627–36.

74. Kang KY, Kang Y, Kim M, Kim Y, Yi H, Kim J, Jung HR, Park SH, Kim HY, Ju JH, Hong YS. The effects of antihypertensive drugs on bone mineral density in ovariectomized mice. J Korean Med Sci. 2013;28(8):1139–44.
75. Faot F, Chatterjee M, de Camargos GV, Duyck J, Vandamme K. Micro-CT analysis of rodent jaw bone micro-architecture: a systematic review. Bone Rep. 2015;2:14–24.
76. Tanaka M, Ejiri S, Kohno S, Ozawa H. Region-specific bone mass changes in rat mandibular condyle following ovariectomy. J Dent Res. 2000;79:1907–13.
77. Rhee Y, Hur JH, Won YY, Lim SK, Beak MH, Cui WQ, Kim KG, Kim YE. Assessment of bone quality using finite element analysis based upon micro-CT images. Clin Orthop Surg. 2009;1(1):40–7.
78. Parashar SK, Sharma JK. A review on application of finite element modelling in bone biomechanics. Perspect Sci. 2016;8:696–8.
79. Christen P, Schulte FA, Zwahlen A, van Rietbergen B, Boutroy S, Melton LJ III, Amin S, Khosla S, Goldhahn J, Müller R. Voxel size dependency, reproducibility and sensitivity of an in vivo bone loading estimation algorithm. J R Soc Interface. 2015;13:1–8.
80. Barak MM, Black MA. A novel use of 3D printing model demonstrates the effects of deteriorated trabecular bone structure on bone stiffness and strength. J Mech Behav Biomed Mater. 2018;78:455–64.
81. Particelli F, Mecozzi L, Beraudi A, Montesi M, Baruffaldi F, Viceconti M. A comparison between micro-CT and histology for evaluation of cortical bone: effect of polymethylmethacrylate embedding on structural parameters. J Microsc. 2011;245(3):302–10.
82. Tiede-Lewis LM, Xie Y, Hulbert MA, Campos R, Dallas MR, Dusevich V, Bonewald LF, Dallas SL. Degeneration of the osteocyte network in the C57BL/6 mouse model of aging. Aging. 2017;9(10):2190–208.
83. Pazzaglia UE, Zarattini G, Giacomini D, Rodella L, Menti AM, Feltrin G. Morphometric analysis of the canal system of cortical bone: an experimental study in the rabbit femur carried out with standard histology and micro-CT. Anat Histol Embryol. 2010;39(1):17–26.
84. Britz HM, Jokihaara J, Leppanen OV, Jarvinen T, Cooper DML. 3D visualisation and quantification of rat cortical bone porosity using a desktop micro-CT system: a case study in tibia. J Microsc. 2010;240:32–7.
85. Gur A, Nas K, Kayan O, Atay MB, Akyuz G, Sindal D, Adam M. The relation between tooth loss and bone mass in postmenopausal osteoporotic women in Turkey: a multicenter study. J Bone Miner Metab. 2003;21(1):43–7.
86. Jeffcoat M. The association between osteoporosis and oral bone loss. J Periodontol. 2005;76:2125–32.
87. Ejiri S, Tanaka M, Watanabe N, Anwar RB, Yamashita E, Yamada K. Estrogen deficiency and its effect on the jaw bones. J Bone Miner Metab. 2008;26(5):409–15.
88. Lee MM, Chu EY, El-Abbadi MM, Foster BL, Tompkins KA, Giachelli CM, Somerman MJ. Characterization of mandibular bone in a mouse model of chronic kidney disease. J Periodontol. 2010;81:300–9.
89. Guo Y, Sun N, Duan X, Xu X, Zheng L, Seriwatanachai D, Wang Y, Yuan Q. Estrogen deficiency leads to further bone loss int he mandible of CDK mice. PLoS One. 2016;11(2):e0148804. https://doi.org/10.1371/journal.pone.0148804.
90. Johnston BD, Ward WE. The ovariectomized rat as a model for studying alveolar bone loss in postmenopausal women. Biomed Res Int. 2015;2015:635023. https://doi.org/10.1155/2015/635023.